Milton E. Cram, W8NUE
9807 Vista View, Austin, TX 78750; **w8nue@arrl.net**

Small Transmitting Loops: a Different Perspective on Tuning and Determining *Q* and Efficiency

The simplest way to tune and match the loop antenna is by using the Smith chart, and Q can be estimated using the complex impedance.

Over the past several decades numerous articles have been published[1-7] that describe the construction and testing of small transmitting loop antennas. "Small" in this context refers to an antenna that has a circumference that is less than about a tenth of a wavelength. In this article I focus more on evaluation of the performance of the antenna and less so on the construction aspects. I rely on both models and measurements on a simple loop antenna. To my knowledge, there have been no articles that describe the method of matching a loop or of determining the *Q* of the antenna as presented herein. I do not attempt to cover electromagnetic theory, or modeling using such tools as NEC. The notes describe construction methods, NEC models, and so on. This is a *phenomenological* approach, where it is assumed that the current distribution in the loop is constant and the behavior is adequately described using a simple RLC circuit.

My purpose is to:

- describe the electrical behavior of a small transmitting loop antenna near the tuned frequency using an electrical circuit analog;
- provide guidance in tuning the antenna for an impedance match to a coaxial transmission line;
- describe a measurement method for determining the *Q* of the antenna system;
- estimate the efficiency of the antenna based on measured *Q*;
- compare model data with data obtained from measurements.

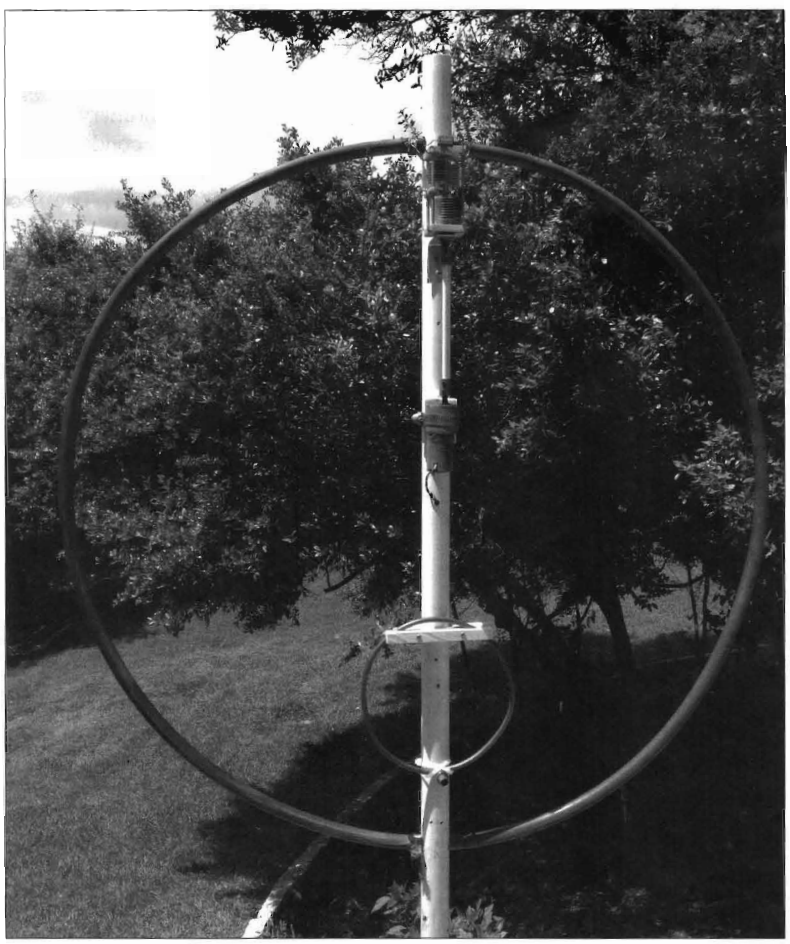

Figure 1 — The small transmitting loop antenna includes the main loop with the resonating capacitor on top, and the feeding loop near the bottom. [Milton Cram, W8NUE, photo.]

Assumptions

The circumference of the loop is assumed small compared to wavelength, that is, current is essentially constant around the loop. For a more accurate current distribution, see reference[8-10] by Siwiak, Findling and Quick. The coax cable is connected to a small coupling loop that is inductively coupled to the main loop. This analysis should also apply to "delta" and "gamma" matching systems.

The loop antenna (Figure 1) to be examined is one that I built several years ago for PSK31 operation on 20 meters. The main loop is approximately 32 inches in diameter, and is constructed from 5/8 inch OD copper tubing. A butterfly capacitor is connected across the gap formed where the length of copper tubing is shaped into a loop. This capacitor resonates the loop at 14.1 MHz. A small 7.75 inch diameter feeding loop, formed from 0.25 inch OD copper tubing, transfers power into and out of the main loop. A 50 Ω coax cable connects across the gap that is formed when the tubing is shaped into the smaller feeding circular loop.

The position of the small coupling loop is used to alter the mutual inductance, or coupling coefficient, between the two loops, and this provides a means to adjust the matching between the coax and the antenna for a 1:1 VSWR.

Although the butterfly capacitor may not have losses as low as a vacuum variable capacitor, it is what I had available. Likewise, losses in the loop would be lower with a larger diameter main loop conductor. Improvements would be possible if more attention were paid to reducing losses in the system.

While the purpose of his article is not to describe the design and construction of small transmitting loop antennas, my description and Figure 1 should enable anyone to replicate the evaluation that I have done. There are numerous articles available from the internet, and other sources, to guide one in building such an antenna. Be warned that there are many misleading claims about such antennas — such as claims of "efficiency greater than 90% on 80 and 40 meters", and there are errors in some of the formulas.

Circuit Model

I assume that the loop antenna can be modeled using a simple first-order system electronic circuit analog. That is, the antenna is equivalent to a transformer with a series RC circuit across the secondary of the transformer. Such a model (Figure 2) has also been suggested by others[11]. A detailed analysis of this circuit model can provide very useful information for both the adjustment of the antenna for proper match to the feed line, and in estimating the efficiency of the antenna.

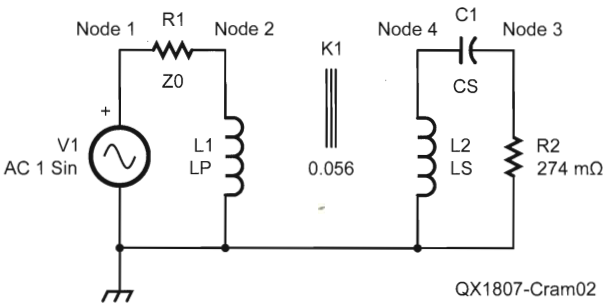

Figure 2 — A TopSpice model of the small transmitting loop antenna. Spice parameters are: Z0 = 50 Ω; LP = 0.434 μH; LS = 2.05 μH, CS = 62.55 pF; W0 = {1/SQRT(LS*CS)}; XLP = {W0*LP/Z0}; R2 = 274 mΩ.

The *primary* of the transformer is the *small coupling loop* to which the transmission line is connected. The *main loop* of the antenna is the *secondary* of the transformer, loaded with a resistor and capacitor. The inductance L (henry) of a single turn loop is,

$$L = \mu_0 b \ln\left(\frac{8b}{a} - 2\right) \quad (1)$$

where μ_0 is the permeability of free space, b is the radius of the loop in meters, and a is the radius of the conductor in meters.

In my model the primary inductance is 0.434 μH, and the secondary inductance is 2.05 μH. The resonating capacitance at 14.1 MHz is 62.5 pF. The secondary resistance includes the radiation resistance of the antenna *and* the effect of all losses in the antenna system, such as the resistive losses in the antenna materials, ground and other nearby lossy materials. I set the value for the total resistance to 0.27 Ω based on measured data (explained later). With these values of resistance and the inductances the simulations are in close agreement with measurements.

I analyzed the circuit in Figure 2, with the free demo Version 8 of *TopSpice* (**www.penzar.com**). I chose this application because of its ability to generate Smith charts. The demo version is limited in the number of components and nodes, but suffices for this simple model.

To gain further insight into the model, I also derived the equations that apply to the circuit. The input impedance to the antenna, at the point the coax is connected to the coupling loop is,

$$Z_{in}(\omega) = j\omega L_p + \frac{(\omega M)^2}{Z_s(\omega)} \quad (2)$$

where the series impedance of the secondary is,

$$Z_s(\omega) = R_s + j\omega L_s + \frac{1}{j\omega C_s} \quad (3)$$

L_p is the inductance of the coupling loop, L_s is the inductance of the main loop, C_s is the resonating capacitance, and includes any stray capacitance. Resistance R_s accounts for all power loss in the antenna system, including radiation loss. To more easily understand the behavior of the antenna near resonance, I have used a change of variables in the equation for the input impedance. I have also employed the commonly used expression for the Q of the tuned circuit.

The mutual inductance between the primary and secondary will be represented by the coupling coefficient k using the formula,

$$M^2 = k^2 L_p L_s \quad (4)$$

The resonant frequency of a series tuned circuit is,

$$f_0 = \frac{1}{2\pi\sqrt{L_s C_s}}$$

and Q is,

$$Q = \frac{2\pi f_0 L_s}{R_s}$$

Since we are interested in the behavior of the antenna near its resonant frequency, we make the substitution $f = f_0(1+\delta)$, where $|\delta| << 1$. Without going into the detailed manipulation, the input impedance is,

$$Z_{in}(\delta) = j\omega_0 L_p(1+\delta) + \frac{\omega_0^2 M^2 (1+\delta)^2}{Z_s(\delta)} \quad (5)$$

where the series impedance of the secondary is,

$$Z_s(\delta) = R_s + j\omega_0 L_s(1+\delta) + \frac{1}{j\omega_0 C_s(1+\delta)} \quad (6)$$

Using the common definition of Q, the equation for the input impedance can be simplified to,

$$Z_{in}(\delta) = j\omega_0 L_p(1+\delta)+(1+2\delta)k^2Q(1+2\delta Q) \quad (7)$$

Because $|\delta| << 1$, we made the substitution $(1+\delta)^2 = 1+2\delta$, and $1/(1+\delta) = 1-\delta$. This introduces negligible error. As you will see later, the calculated impedance matches measured data very closely. These approximations imply that we have a high Q system.

Eqn. (7) is used to examine the real and imaginary parts of the input impedance as a function of the deviation of the frequency from the self-resonant frequency of the loop. The frequency deviation is δf_0.

The real part of $Z_{in}(\delta)$ is,

$$\mathrm{Re}\{Z_{in}(\delta)\} = \frac{\omega_0 L_p(1+2\delta)k^2Q}{(1+4\delta^2Q^2)} \quad (8)$$

and the imaginary part of $Z_{in}(\delta)$ is,

$$\mathrm{Im}\{Z_{in}(\delta)\} = \omega_0 L_p\left((1+\delta)-\frac{(1+2\delta)2\delta k^2Q^2}{(1+4\delta^2Q^2)}\right) \quad (9)$$

At resonance, we satisfy two conditions,

$$\mathrm{Re}\{Z_{in}(\delta)\} = Z_0 \quad (10)$$

$$\mathrm{Im}\{Z_{in}(\delta)\} = 0 \quad (11)$$

where Z_0 is the characteristic impedance of the coax transmission line, nominally 50 Ω. From the condition on the real part we have

$$\frac{\omega_0 L_p(1+2\delta)k^2Q}{(1+4\delta^2Q^2)} = Z_0 \quad (12)$$

re-written as,

$$\frac{(1+2\delta)k^2Q}{(1+4\delta^2Q^2)} = \frac{Z_0}{\omega_0 L_p}. \quad (13)$$

If we now insert expression (13) into (9) for the imaginary part of $Z_{in}(\delta)$ we obtain

$$\mathrm{Im}\{Z_{in}(\delta)\} = \omega_0 L_p\left((1+\delta)-\frac{2\delta QZ_0}{\omega_0 L_p}\right) \quad (14)$$

Setting this expression to 0, as required for resonance,

$$\delta_{res} = \frac{1}{\frac{2QZ_0}{\omega_0 L_p}-1} \quad (15)$$

When the frequency f is $f_0(1+\delta_{res})$, the real part of the impedance is Z_0 and the imaginary part is 0. That is, *resonance occurs at a frequency different from that where the reactance of the main loop is zero.*

We now return to the Eqn. (8) for the real part of the impedance to determine what coupling coefficient is needed to achieve Z_0 ohms for the real part. After some manipulation we obtain,

$$k^2 = \frac{Z_0\left(1+4\delta_{res}^2Q^2\right)}{\omega_0 L_p\left(1+2\delta_{res}\right)Q} \quad (16)$$

In practice, we do not have to solve this equation for the coupling coefficient as we usually adjust the coupling to achieve the desired resonance condition using either an impedance analyzer, or a VSWR bridge. However, it may be enlightening to make the calculation once we have an estimate of the Q.

Determination of the antenna Q

The Q of the antenna is of interest for two main reasons. First, the usable bandwidth (without the need for retuning) is determined by the Q and second, the efficiency of the antenna is dependent on Q.

It has been proposed[12] that the Q of an RLC circuit can be determined from VSWR measurements. I have confirmed mathematically, using this circuit model, that VSWR measurements can indeed be used to estimate the Q. However, for the method to work, the VSWR must be very close to 1:1 at the operating frequency. When this condition is met, if one determines frequencies on either side of resonance where the VSWR reaches a specific level, the difference in frequencies at the specified VSWR level, divided into the frequency at 1:1 VSWR provides a number that is proportional to the Q of the antenna. For a target VSWR of 2.618, the proportionality constant is 1.

Since using the VSWR method to determine Q requires a good match, I decided to look at an alternative method. Using plots (Figure 3) of the real and imaginary part of Z_{in} obtained from the *TopSpice* model, it is obvious that changes in the coupling coefficient between the small and large loops have a very small effect on the frequencies at which the imaginary part of Z has its

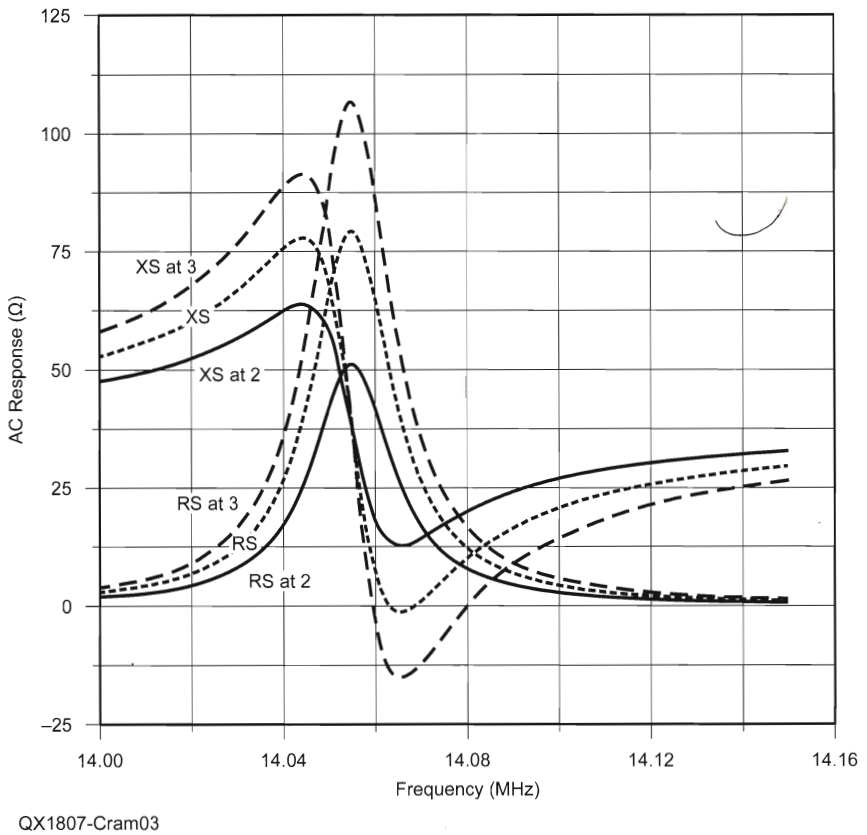

Figure 3 — R and X plots for the small transmitting loop tuned to approximately 14.07 MHz.

maximum and minimum values (close to the resonant frequency f_0). This led me to further analyze the expression for the imaginary part of Z_{in} in the vicinity of f_0.

Recall Eqn. (9) for the imaginary part of $Z_{in}(\delta)$. Since δ is very small, we can approximate $\mathrm{Im}\{Z_{in}(\delta)\}$ with,

$$\mathrm{Im}\{Z_{in}(\delta)\} = \omega_0 L_p \left(1 - \frac{2\delta k^2 Q^2}{(1+4\delta^2 Q^2)}\right) \tag{17}$$

We then differentiate this expression with respect to δ and set the derivative to zero to locate the maximum and minimum values as a function of δ. This yields the result that when $\delta = \pm 1/2Q$, the imaginary part of the input impedance will have either a maximum or minimum value. Pursuing this further, we focus on the *TopSpice* model results.

Figure 3 is an output from the *TopSpice* program showing the behavior of the real and imaginary parts of the input impedance close to the resonant frequency f_0. The three sets of plots in the above figure correspond to three different values of coupling coefficient. It is particularly interesting that the location in frequency of the maximum and minimum values of the imaginary (X) part of the impedance do not appear to move as the coupling coefficient is changed, as suggested earlier. This tends to confirm that the previous analysis is a valid means to calculate the Q. That is, we can use the expression

$$Q = \frac{f_0}{|f_{\max} - f_{\min}|} \tag{18}$$

where

$$f_{\max} = f_0\left(1 + \frac{1}{2Q}\right) \text{ and } f_{\min} = f_0\left(1 - \frac{1}{2Q}\right)$$

If we further examine the plots, we find that on the middle (R, X) set, X is zero very close to 14.07 MHz and R is very close to 50 Ω. When the coupling coefficient is reduced, X never passes through zero, so there can be no resonance. When the coupling coefficient is increased, we again have two frequencies for which X is zero, but now the R value is either too high, or too low. Consequently, there is only one value of coupling coefficient that achieves perfect match. VSWR is not a good way to determine if coupling needs to be increased or decreased since VSWR can be too high because the transformed impedance is either too high or too low.

To further demonstrate the effect of coupling coefficient changes on the input impedance, I used the *TopSpice* model to generate Smith Chart plots seen in Figure 4. Only the center curve passes through the center of the Smith chart where $R = 50\ \Omega$ and $X = 0$. This corresponds to a VSWR of 1:1, or a reflection coefficient of zero.

This figure demonstrates that if one uses an impedance analyzer that is capable of plotting a Smith chart, it is easy to determine which way the coupling must be changed to achieve a perfect match. The upper curve (solid line) requires an increase in coupling, while the lowest curve (large dashes) requires a decrease in coupling. Such a conclusion is not obvious when using the impedance or VSWR plot.

Note the point labeled ZLS at the top of the Smith chart. This point represents the normalized impedance $j\omega_0 L_p$ of the primary (feeding) loop at f_0. Each of the circular plotted curves appear to be tangent to the outer circle of the Smith chart at ZLS.

Efficiency

Low-power operators are especially interested in the efficiency of their antenna systems. In this section, I will provide some estimates of antenna efficiency based on measurements using a Vector Impedance Analyzer (VIA).

The rationale for my determination of efficiency is that the effective series resistance R_{eff} of the loop antenna adequately accounts for all power losses, including the radiated power. Ideal inductors and capacitors can store energy, but over a complete cycle of the RF, dissipate no power. In this analysis, the losses in the inductor and capacitor are lumped into the single resistance R_{eff}. Furthermore, this effective resistance is related to the Q as noted earlier. It is also generally accepted that the radiation resistance, which is part of the effective resistance, represents power that is radiated by the structure.

The radiation resistance[13] is about,

$$R_{rad} = 197 C_\lambda^4 \tag{19}$$

where C_λ is the circumference of the loop in wavelengths. Siwiak and Quick discuss an improved formula[14] for radiation resistance that includes the effects of non-uniform

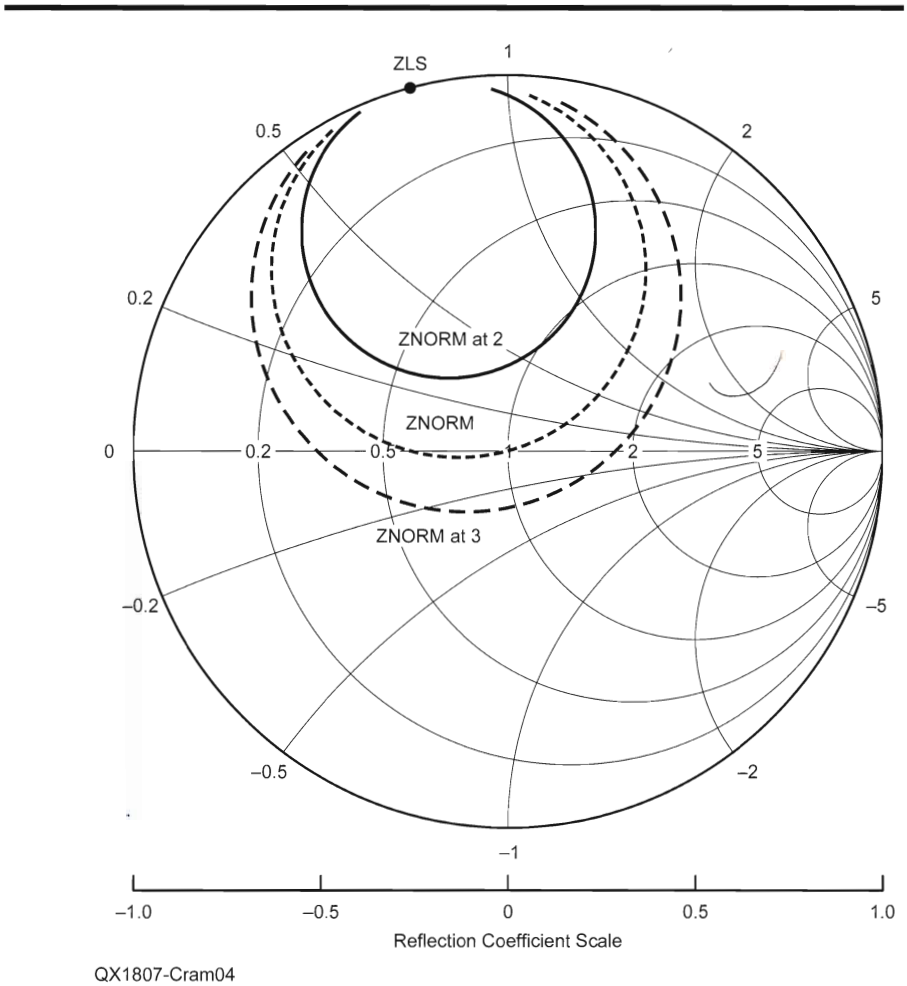

Figure 4 — Smith chart plots for three different coupling coefficient values.

current in the loop.

Allow I_{rf} to represent the rms RF current that flows in the loop. The total power that is dissipated in the loop is,

$$P_{total} = I_{rf}^2 R_{eff} \tag{20}$$

and the power radiated is,

$$P_{rad} = I_{rf}^2 R_{rad} , \tag{21}$$

the radiation efficiency is therefore,

$$efficiency = 100\% \frac{P_{rad}}{P_{total}} = 100\% \frac{R_{rad}}{R_{total}} \tag{22}$$

The Q of the antenna is,

$$Q = \frac{\omega L_s}{R_{eff}} \tag{23}$$

where R_{eff} is the same as R_s in the *TopSpice* model. We can also express efficiency as

$$efficiency = 100\% \frac{R_{rad} Q}{\omega L_s} \tag{24}$$

This shows that the only options we have for increasing efficiency is to increase R_{rad} or Q. R_{rad} can be increased by making the loop larger, and Q may be increased by using lower-loss materials.

Measurements on Small Loop Antenna

Next we discuss measurements using a Vector Impedance Analyzer (VIA), like the one offered by the Austin Texas QRP group (**www.qsl.net/k5bcq/Kits/Kits.html**). The VIA is first calibrated using a short piece of 50 Ω coax between the VIA and the open, short, and calibration resistor. This makes the measurement point at the end of the coax, away from the VIA.

The antenna is initially set with the plane of the small loop parallel to the plane of the main loop. The small coupling loop is positioned so that no point on its circumference is closer to the main loop than about 1 inch. Also, see Figure 1, the coupling loop is mounted diametrically opposite from the tuning capacitor.

A VSWR scan is then run over a wide frequency range (Figure 5) to determine the approximate tuned frequency. The tuning capacitor is then adjusted to set the operating frequency of the antenna as close to 14.1 MHz as possible. The scan range of the VIA is reduced to a few hundred kilohertz, as in Figure 6. We then scan the new range and use the Smith chart plot option (Figure 7) on the VIA. Note the similarity to the traces of Figure 4. This plot reveals whether the coupling between the small and large loops is too little or too much. If the plot does not encircle the center of the chart, then the coupling is too small. If the plot encircles the chart center, then the coupling is too much. The movable cursor in the VIA plot has been placed at the VSWR minimum, to allow readout of the corresponding frequency.

Since the magnetic field due to the main loop current is strongest immediately adjacent to the conductor and weakens towards the center of the loop, moving the small coupling loop closer to the main loop will increase the coupling coefficient. Likewise, moving the small coupling loop closer to the center of the main loop will reduce the coupling coefficient. The coupling coefficient can also be reduced by rotating the plane of the small loop so that it is no longer parallel to the plane of the main loop.

In Figures 8 and 9 the display cursor has been placed over the maximum and minimum points on the reactance curves (upper traces). The corresponding frequencies are 14,078,996 and 14,100,313 Hz. The difference between these two values is 21,300 Hz. Since the tuned frequency is (Figure 6) about 14,098,000 kHz, the calculated Q is 14,098,000/21,300, or 662.

We now calculate R_{rad} and L_s using Eqns. (19) and (1), respectively, and use the measured Q as described above to provide an estimate of the efficiency of the antenna. For the 32 inch loop, $R_{rad} = 0.04\ \Omega$. The $Q = 660$, and $L_s = 2.05\ \mu H$. At 14.1 MHz, this value of Q gives $R_{eff} = 0.274\ \Omega$ yielding an efficiency of about 14.5% (or -8.4 dB). This is the value of R_{eff} that I used in the circuit model.

Note in Figure 7 the point where the circular loop is tangent to the outer circle of the Smith chart is very close to the corresponding point in Figure 4. This indicates that the calculated and measured coupling loop inductances are in very close agreement. Finally, Figure 10 shows the measured reflection coefficient (V-shaped trace, left side scale) and its phase (trace starts on the left just above 90°using the right side scale).

Closing Comments.

The effective loss resistance R_{eff} of the loop can be found from the measurement of Q, which is assumed to include *all* power losses, including radiation loss. The calculated radiation resistance R_{rad} is based on an ideal determination of the loss due to radiated power. Consequently, calculation of efficiency using R_{eff} and R_{rad} will produce a value for efficiency subject to how accurately R_{rad} represents the radiation resistance. Q must be relatively high for the approximation $\delta << 1$ to hold true, hence this analysis may

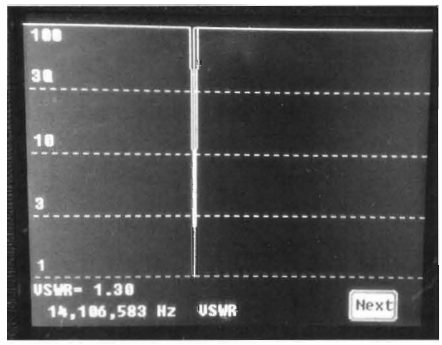

Figure 5 — Broad band VSWR Scan (10 to 20 MHz) to locate resonance.

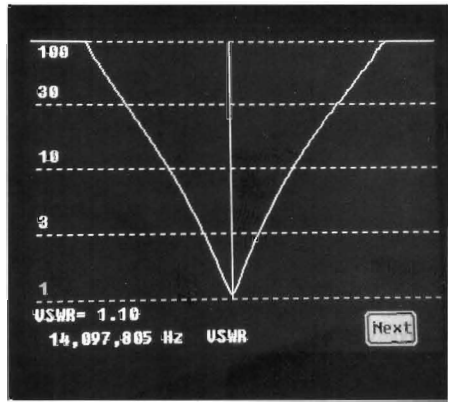

Figure 6 — Narrow band, 14.0 to 14.2 MHz, measured VSWR scan.

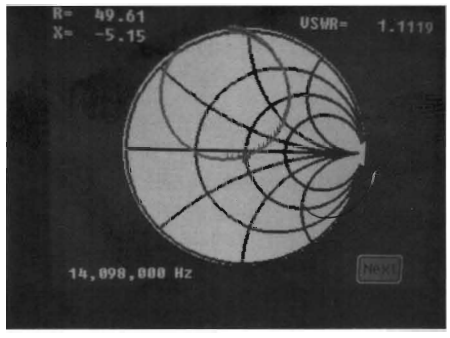

Figure 7 — The narrow band, 14.0 to 14.2 MHz, scan presented as a Smith chart. The cursor is shown at 14,098,000 kHz, the point of minimum VSWR.

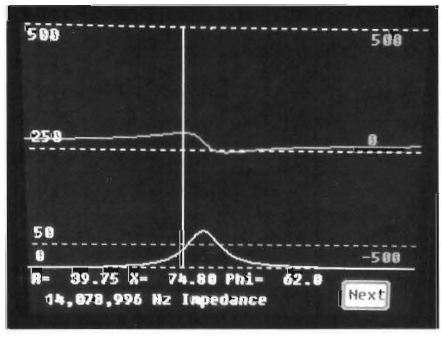

Figure 8 — Impedance plot showing maximum reactance on the upper trace. Lower trace is resistance.

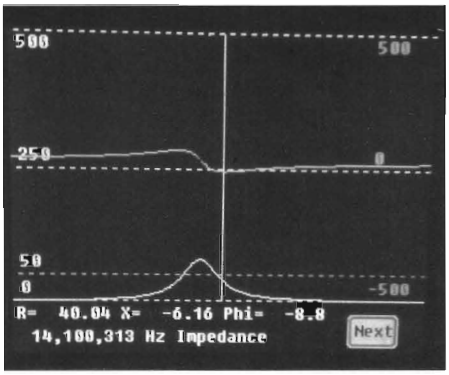

Figure 9 — Impedance plot showing minimum reactance, upper trace. Lower trace is resistance.

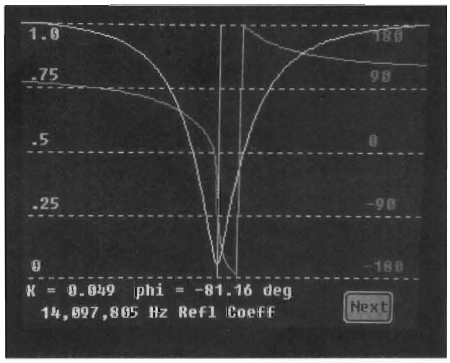

Figure 10 — Measured reflection coefficient magnitude (V-shaped trace, left-edge scale) and its phase (trace starts and ends near 90 on the right-edge scale).

$\delta << 1$ to hold true, hence this analysis may not produce accurate results when the Q is low (<100).

Regarding radiation resistance, I used the simplified Eqn. (19), which ignores the effects of non-uniform current in the loop, or any effects from the *E*-field present in the gap where the tuning capacitor is located. Only the far *electric* and *magnetic* fields due to a perfectly constant loop current are involved in deriving Eqn. (19). Some radiated power might couple to objects close to the antenna. The effect of such power loss is included in R_{eff}.

Conclusions

We have shown that the simple circuit model, with an appropriate choice of parameters, produces results that closely match measured data from a test loop antenna. Using a VIA we have obtained measured data from a small-diameter copper-tubing loop ($C_\lambda = 0.12$), that are in very good agreement with *TopSpice* circuit analysis simulations.

I have presented a method for using the plotting features of a VIA to facilitate adjustments to the antenna for correct impedance matching. In addition to VSWR and impedance plots, the Smith chart presentation of the measurements is a straightforward method for adjusting the coupling to the antenna. There is no guessing as to which way to adjust coupling for impedance matching.

VIA plots of the complex input impedance allow a simple means to determine the Q of the antenna. From this Q, and the calculated inductance of the loop, and the operating frequency, one can easily estimate an upper limit on the efficiency of the antenna. As shown in this example the efficiency is slightly less than 15%.

Milton E. (Milt) Cram, W8NUE, was first licensed in 1953 and holds an Amateur Extra Class license, and is a member of ARRL and QRP ARCI. He earned the BS, MS, and PhD degrees in Electrical Engineering from Georgia Tech. He has many years of experience in the automotive, oil and gas service industry, nuclear power instrumentation, and military electromagnetics applications, and holds patents in each of those areas. Milt is active in the Austin TX QRP Club and has contributed to several projects that have been offered by the club — most recently, the Vector Impedance Analyzer kit. He has published articles in QST and QEX on touch paddle keys, and the NUE-PSK digital modem. He is currently retired and living in Austin TX, where he continues to design projects for the ham community.

Notes

[1]Steve Yates, AA5TB, small loop calculator, **www.aa5tb.com/loop.html**.
[2]Glen E. Gardner, Jr., AA8C, Loop antenna, **gridtoys.com/glen/loop/loop3.html**.
[3]Small transmitting loop, **owenduffy.net/blog/?p=4888**.
[4]Carol F. Milazzo, KP4MD, "14-30 MHz Magnetic Loop, Antenna", **www.qsl.net/kp4md/magloophf.htm**.
[5]Small transmitting loop, **https://www.nonstopsystems.com/radio/frank_radio_antenna_magloop.htm**.
[6]John S. Belrose, "Performance of Electrically Small Tuned Transmitting Loop Antennas" *Radcom, Radio Society of Great Britain*, London, UK, June/July, 2004.
[7]Mike Underhill, "Small Loop Antenna Efficiency" Presented in Kempton UK, May 2006,
[8]A. Findling, K9CHP and K. Siwiak, KE4PT, "How Efficient is Your QRP Small Loop Antenna?", *QRP Quarterly*, Summer 2012.
[9]K. Siwiak, "Loop Antennas," in John G. Proakis (Ed.), **Wiley Encyclopedia of Telecommunications**, New York, NY: John Wiley & Sons, 2002, pp. 1290-1299.
[10]K. Siwiak and R. Quick, "Small Gap-resonated HF Loop Antenna Fed by a Secondary Loop", *QEX*, Jul./Aug., 2018, elsewhere in this issue.
[11]Alan Boswell, Andrew J. Tyler, and Adam White, "Performance of a Small Loop Antenna in the 3-10 MHz Band", *IEEE Transactions on Antennas and Propagation*, Vol. 47, No. 2Apr., 2005, pp. 51-56.
[12]A. D. Yaghjian and S. R. Best, "Impedance, Bandwidth and Q of Antennas," *IEEE International Symposium on Antennas and Propagation Digest*, 1, Columbus, Ohio, June 2003, pp. 501-504.
[13]J. Kraus, Chapter 6, **Antennas**, McGraw Hill, 1950.
[14]K. Siwiak and R. Quick, op. cit., Note 10.

Peter DeNeef, AE7PD
2033 Abby Gate Dr., Roseville, CA 95747; **hamradioandvision@gmail.com**

Effects Due to Ground For Small Transmitting Loop Antennas

The location of the resonating capacitor and coupling to earth ground affect the loop pattern and gain.

Amateurs often place small transmitting loop antennas close to the ground for convenient tuning, for portability, or because of local antenna restrictions. I used computer simulations of a typical Amateur Radio HF loop to learn the effects of height above ground on the gain and antenna patterns.

Early in the development of the Numerical Electromagnetics Code (NEC), G.J. Burke noted unstable results with models of electrically small loops. When there is little variation in the standing wave current on a loop, a small change in frequency can change the calculated admittance by orders of magnitude. He concluded[1], "For a loop over a finitely conducting ground the solution fails when the loop size is somewhat less than resonant. Hence small loops over ground cannot presently be modeled". In a 2015 e-mail Dr. Burke wrote to me that improvements in the NEC over the years do not resolve this issue for modeling small loops.

At 7 MHz a 1 meter loop is electrically small ($C_\lambda = 0.07$), where C_λ is the circumference in wavelengths. The variation in the current distribution[2, 3] around the loop is just 2% at 7 MHz, so results from NEC simulations are open to question. Until recently, testing NEC simulations for electrically small loops over lossy media has been problematic. In 2014, Austin, *et al.*, demonstrated a technique[4] for comparing NEC results to theoretical predictions of the input impedance. As described in "Accuracy Tests" below, NEC simulations for a 1 meter diameter loop at 7 MHz agree with this theory, validating the calculations.

Antenna Patterns

I used an NEC-2 model in EZNEC[5] for a vertical 1 m diameter loop of 10 mm (3/8 inch) diameter copper tubing located above "good" ground[6] (conductivity σ = 7 mS/m and relative permittivity ε_r = 17). A voltage source is at the bottom of the loop, and a lossless tuning capacitor is across the gap at the top.

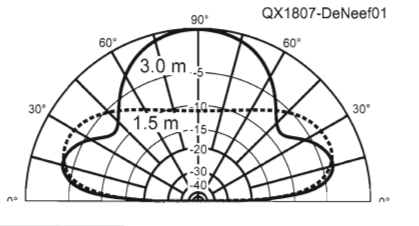

Figure 1 — Elevation plots for loops 1.5 m and 3.0 m above ground at 29 MHz. The resonating capacitor is at the top of the loop. Outer circle is 4.5 dBi.

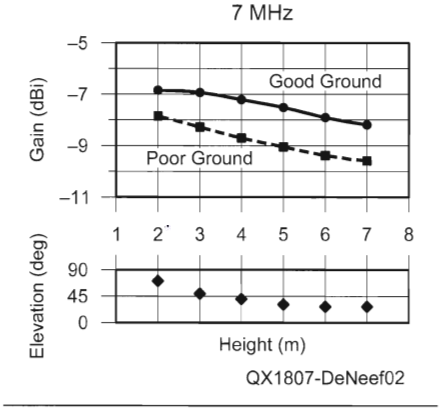

Figure 2 — For 7 MHz, maximum gain and elevation angles vs. height.

Figure 1 shows elevation plots at 29 MHz for two loops — one with a center-height of 1.5 m, and the other at 3.0 m. The plots are in the plane of the loop, where the gain is highest. The loop mounted closer to the ground has a different radiation pattern and less gain. For the loop at h = 1.5 m the maximum gain is 1.4 dBi at 24° elevation, and at h = 3.0 m it is 4.5 dBi at 90°.

The type of ground has a relatively small effect on the gain of this loop. Figures 2 – 5 show the maximum gain *vs.* height for 7, 14, 21, and 29 MHz, respectively. The solid lines show the gain with good ground as specified above, and the dashed lines are with very "poor" ground (σ = 1 mS/m, ε_r = 5). A chart under each graph shows the elevation angle at maximum gain for the "good" ground. The elevation plots represented by Figures 2 – 5 are available from the **www.arrl.org/QEXfiles** web page.

7 MHz

Figure 2 shows gain decreasing slowly as the height increases. The elevation at maximum gain also decreases, but the patterns are so wide (large 3 dB beamwidth) that for practical purposes the plots are similar from 2 m to 5 m. The figure does not show data for heights below 2 m because, as discussed below, NEC simulations for 7 MHz are less accurate for loops below this height. Theoretical predictions for the impedance at this frequency show that the resistance effect of ground increases rapidly below 2 m.

14 MHz

Figure 3 shows gain increasing slowly with height between 1 m and 2 m, and the wide elevation patterns are all similar in this range. For h from 3 m to 5 m, radiation is restricted to lower elevations. At $h = 6$ m the elevation plot has two lobes: at 90° and 18°.

21 MHz

Figure 4 shows that, unlike the previous two bands, gain increases rapidly as the height increases. At 4 m and above, the radiation pattern shifts upward as a new lobe develops at 90° elevation.

29 MHz

Figure 5 shows gain increasing with height up to 4 m. Compared with the plots for 21 MHz, the low-angle lobe at 1 m to 2 m is narrower, and the transition to upward radiation occurs at $h = 3$ m.

Capacitor Location

Kai Siwiak, KE4PT, analyzed (see Siwiak, KE4PT) the electric field that surrounds the loop, and especially around the tuning gap, of a small loop and he observes that the location of the capacitor can affect the pattern of radiation. Figure 6 shows an elevation plot at 29 MHz for two loops at a height of 3 m. With the capacitor at the bottom of the loop the radiation pattern is different from the loop with the capacitor at the top seen in Figure 1. At this frequency the pattern with the capacitor at the bottom is more like that of a loop at $h = 1.5$ m with the capacitor at the top (Figure 1). The elevation plots on the **/QEXfiles** web page are shown for both configurations.

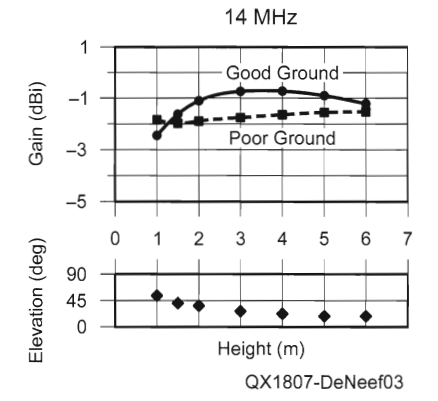

Figure 3 — For 14 MHz, maximum gain and elevation angles vs. height.

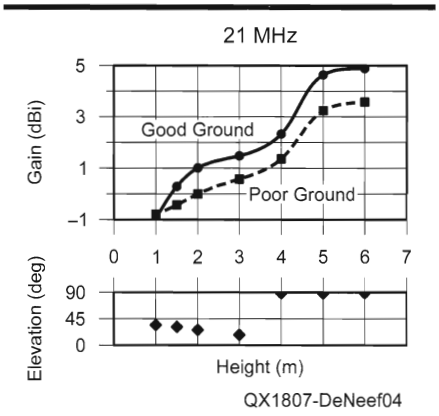

Figure 4 — For 21 MHz, maximum gain and elevation angles vs. height.

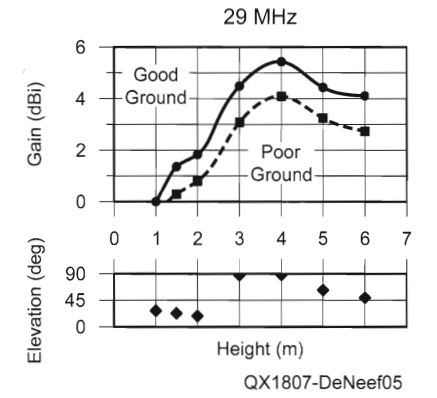

Figure 5 — For 29 MHz, maximum gain and elevation angles vs. height.

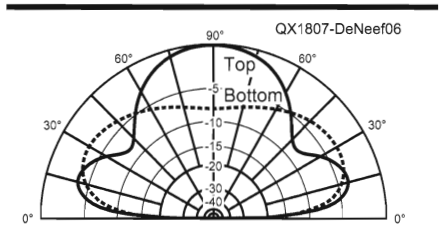

Figure 6 — Elevation plots with the capacitor at the top or bottom of a loop at h = 3 m at 29 MHz. Outer circle is 4.5 dBi.

Accuracy Tests

In addition to the standard accuracy tests for NEC calculations — Average Lossless Gain and Convergence — I used these tests:

1. Comparisons with the Theory Used by Austin et al.

The input resistance of the loop (see Austin *et al.*, and Vogler *et al.*) is $R = R_f + R_g$, where R_f is the radiation resistance of the loop in free space, and R_g is ground-loss resistance. The loop conductor and capacitor are assumed lossless. Nomograms in Vogler, *et al.*, enable you to find R_g/R_f. I calculated R_f using a lossless NEC model of the loop in free space with no capacitor. The nomograms for vertical loops are labeled "HMD" (horizontal magnetic dipole) because the dipole moment lies along the axis perpendicular to the loop and is horizontal.

Figure 7 shows comparisons between theory (solid curves) and NEC-2D simulations (data points) for loops at 7, 14, and 21 MHz. The results shown at 7 MHz for a one-meter diameter loop are recalculations for the example in Austin, *et al.* As they noted, the NEC simulations show reasonable agreement with theory when the height is greater than $\lambda/20$.

This theory is for electrically small loops, so I used a 0.5 m diameter loop ($C_\lambda = 0.07$) for the comparisons at 14 MHz, and a 0.25 m diameter loop ($C_\lambda = 0.06$) at 21 MHz. Agreement is poor when $C_\lambda > 0.1$ because the theory does not account for ground coupling by non-uniform components of current on

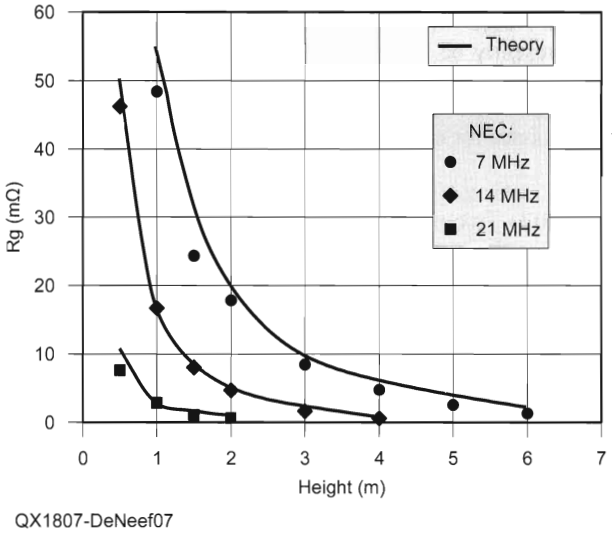

Figure 7 — Comparison of theory and NEC simulations of R_g vs. height for three different electrically small loops.

the loop; the dipole component of current increases as $(2C_\lambda^2)$. I selected realistic ground properties that minimize interpolation error with the nomograms. In each case the index of refraction is $n = 5$, as in Austin *et al.*

NEC simulations of R_g for a 1 m loop show that the effect of ground increases rapidly below $h = 2$ m at 14, 21, and 29 MHz. For 7 MHz the impedance theory predicts a rapid increase in Rg close to the ground ($h < 2$ in Fig. 6).

The calculations also show that R_g $(R - R_f)$ can be negative. R_g is different from the usual definition for ground resistance, which specifically distinguishes the power dissipated in the ground[7].

2. Double-precision (NEC-2D) vs. single-precision (NEC-2)

The unstable NEC results mentioned in the introduction are caused by an ill-conditioned matrix. Small differences between large numbers can cause inaccuracies. With double-precision computation the problem shifts to a lower frequency (see Burke). There is no significant difference between my NEC-2D and NEC-2 simulations of the antenna patterns. I used NEC-2D for the comparisons of R_g with theory in Figure 7.

3. NEC Admittance

There are no sudden changes in the loop admittance at frequencies around 7, 14, 21, and 29 MHz.

4. Wave Impedance Inside the Loop

At the center of a small loop in free space the magnitude of the ratio of the electric field to the magnetic field is $\eta_0 C_\lambda$, where $\eta_0 = 376.73\ \Omega$ (see Siwiak, KE4PT). I used this relationship to validate NEC calculations when $C_\lambda < 0.2$.

Conclusions

NEC-2 calculations for an HF loop antenna at heights from 1 m to 6 m show that coupling to earth ground affects the antenna pattern and the gain. The effects of good ground and very poor ground are similar in magnitude.

For the range 7 – 29 MHz the gains and elevation patterns for the 7 MHz band are the least affected by the height of a loop. At 21 and 29 MHz the gain and elevation angles increase significantly for heights above 3 or 4 m. The location of the capacitor can make a difference in the loop performance, especially at higher frequencies.

My thanks to Kai, Siwiak, KE4PT, for very helpful answers to my questions about small loops.

Peter DeNeef, AE7PD, received his first license as KF7FPX in 2009. He has written about RF exposure safety for QEX (Nov/Dec, 2017), as well as articles about international RF safety guidelines of the International Commission on Non-Ionizing Radiation Protection (ICNIRP). More of his articles can be found on his popular web site for vision-impaired hams, ***www.HamRadioAndVision.com****.*

Notes

[1]G. J. Burke, "Recent Advances to NEC: Applications and Validation," UCRL Preprint 100651, Mar. 3, 1989, pp. 3 – 4 to 3-8, see: **https://e-reports-ext.llnl.gov/pdf/210389.pdf**.

[2]K. Siwiak and Y. Bahreini, **Radiowave Propagation and Antennas for Personal Communications, 3rd Ed.**, Artech House, Norwood, MA, 2007.

[3]K. Siwiak, KE4PT, "Effect of Small HF Loop Near Fields on Direction Finding," *QST*, July 2015, pp. 63 – 64.

[4]B. A. Austin, A. Boswell, and Michael A. Perks, "Loss Mechanisms in the Electrically Small Loop Antenna", *IEEE Antennas and Propagation Magazine*, Vol. 56, No. 4, Aug. 2014, pp. 142 – 147.

[5]Several versions of *EZNEC* antenna modeling software are available from developer Roy Lewallen, W7EL, at **www.eznec.com**.

[6]L. E. Vogler and J. L. Noble, "Curves of Input Impedance Change Due to Ground for Dipole Antennas," NBS Monograph 72, Jan. 31, 1964, see: **nvlpubs.nist.gov/nistpubs/Legacy/MONO/nbsmonograph72.pdf**.

[7]Robert J. Zavrel, Jr, W7SX, Appendix B in, **Antenna Physics: An Introduction**. Available from your ARRL dealer or the ARRL Bookstore, ARRL item no. 0499. Telephone 860-594-0355, or toll-free in the US 888-277-5289; **www.arrl.org/shop**; **pubsales@arrl.org**.

Kai Siwiak, KE4PT and **Richard Quick, W4RQ**
10988 NW 14th St., Coral Springs, FL 33071; **k.siwiak@ieee.org** 695 Fairway Dr., Plantation, FL 33317; **w4rq@arrl.net**

Small Gap-resonated HF Loop Antenna Fed by a Secondary Loop

Improved formulas for the loop current and loop impedance lead to an accurate determination of close-near-fields, and far field null depths.

The small gap-resonated high frequency circular loop antenna has received much attention in Amateur Radio since John H. Dunlavy, Jr. patented[1] his efficient small loop that can be tuned over wide bandwidths. The now-expired patent spawned a multitude of homebrew loops and several commercial products aimed at hams.

Loop analysis dates back to the earliest days of radio with Pocklington's 1897 paper[2] on the thin wire loop. Later Hallén[3] expanded on the receiving qualities of loops, and Storer[4] studied the impedance of thin wire loops. Loop analysis was generalized[5] by Q. Balzano and one of us, Kai Siwiak, KE4PT, to fat wires giving, among other results, the details of current density along the circumference as well as the cross-section of the loop wire. The results here are derived from the Balzano-Siwiak work, and specialized[6] to electrically small loops. We relied on the Neumann formula[7] to find the mutual coupling between the primary and the secondary feeding loops. We also report on the effects of common mode currents (CMCs) coupling to the feeding coax cable, as well as mutual coupling of the loop to the ground. We verified our analytical results by simulations using Numerical Electromagnetic Code (NEC) models in 4*nec*2 software[8]. Our NEC model includes the primary loop, the secondary feeding loop, a resonating capacitor, and a conductor representing the shield of the coaxial feed line.

We present results rather than lengthy derivations that can be gleaned from the referenced notes. In Section (1) we show the loop current density along the loop circumference and in the cross section, revealing current bunching. In Section (2) we present the loop impedance, including effects of loop wire thickness, and non-uniform loop current. In Section (3) we show the effect of the secondary feeding loop. In Section (4) we provide details about the loop near fields and far-field null filling that are a direct result of considering the non-uniform loop current. In Section (5) we show the effects of loop currents coupling to a coaxial feed line shield. In Section (6) we calculate coupling of the loop to the ground. In Section (7) we determine the loop efficiency. We conclude with a summary in Section (8).

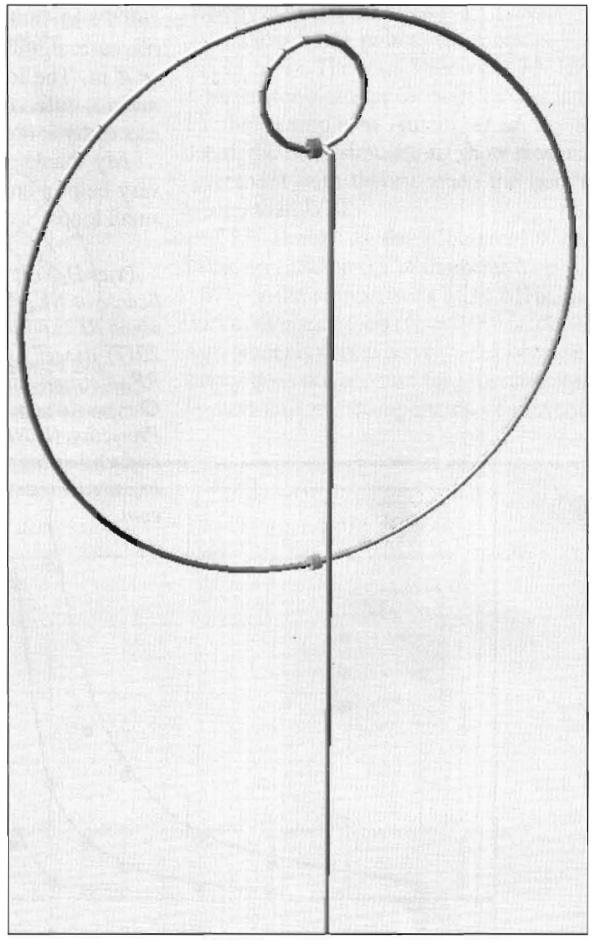

Figure 1 — The electrically small HF loop includes a primary loop and a secondary feeding loop, both in the same *zx*-plane, and a coaxial cable feed line also in the *zx*-plane, but slightly displaced in the *y*-axis, so that the cable does not touch the bottom of the primary loop. A resonating capacitor connects across a gap at the bottom of the primary loop.

1 — Small Loop Currents and Fields

The circular loop geometry for our study is shown in Figure 1, rendered in 4*nec*2 software. The primary loop diameter is 2*b*, the loop

wire diameter is $2a$, the angular extent along the loop circumferences is ϕ, with the loop gap located at $\phi = 0°$. The resonating capacitor is connected across the gap at the bottom of the primary loop. The secondary feeding loop is $2b_2$ in diameter and with $2a_2$ conductor diameter. A coaxial cable feed connects across a gap at the bottom of the smaller secondary loop. We studied the effect of currents coupling to the coax cable shield by varying the length of that coax.

The variation around the loop wire cross-sectional circumference is angle ψ with $\psi = 0°$ pointing to the outside of the loop. We examine a specific loop with $a = 0.00406$ m, $b = 0.4534$ m (loop circumference is 2.85 m), $a_2 = 0.002$ m, and $b_2 = 0.077$ m. The loop centers were displace by 0.343 m. We varied the length of the coax feed line for the common mode current coupling portion of the study. Our loop dimensions closely match those of the *AlexLoop*[9] by Alex Grimberg, PY1AHD.

1.1 — The Dunlavy Loop

John Dunlavy discovered that a loop antenna comprising a one turn primary loop having a circumference of less than three-eighths of a wavelength and interrupted along its length by a gap, with a tuning capacitor connected across the gap, can be tuned by up to a 10:1 tuning range. A single-turn secondary loop, much smaller than the primary loop, is inductively coupled to the primary loop. Both loops are in the same plane. The secondary loop diameter is selected to bear an optimum relationship to the diameter of the primary loop so that variation in feed impedance is minimized over the band of operation. A low impedance transmission line (50 Ω) connects to the terminals of the secondary loop.

Dunlavy used relatively thick conductors of copper or aluminum, and a construction that minimized excessive resistive losses.

1.2 — Loop Current Density

The loop current density $J(\phi, \psi)$ is a Fourier series in terms of $\cos(n\phi)$ along the loop circumference and $\cos(m\psi)$ along the cross-sectional circumference. We initially retained just the $m = n = 0$ and 1 terms. The $m = 1$ term reveals current bunching on the inner surface of the loop conductor. The $n = 1$ term accounts for the first order variation of the circumferential loop current. Including that term reveals details about the close-near fields, and about the far-field peak-to-null ratio. The current density is,

$$J(\phi,\psi) = \frac{I_0}{2\pi a}\left\{1 - 2(kb)^2\cos(\phi)\right\}\left\{1 + Y(a,b)\cos(\psi)\right\} \quad (1)$$

The first curly brackets contain the circumferential variation of the current in ϕ. The second curly brackets include the function $Y(a, b)\cos(\psi)$, which describes current bunching in the cross-sectional circumference of the loop conductor. These curly-bracket terms are ignored in most previous formulas for loop current density. From Note 6 a curve-fit approximation for Y is,

$$Y(a,b) = -\left(\frac{2a}{10a+b}\right)^{0.75} \quad (2)$$

which when multiplied by $\cos(\psi)$ integrates to zero in the ψ-directed cross sectional circumference of the loop conductor. In our example values of a and b, $Y = -0.046$, indicating less than 5% current bunching on the inner surface of the loop conductor. Since our loops have an a to b ratio of less than 0.009, we will not consider the current bunching in the ψ direction any further.

Integrating the current density over the loop conductor cross section in ψ, and noticing that the circumference in wavelengths $kb = 2\pi b/\lambda = C_\lambda$, we see that the loop current is,

$$I(\phi) = I_0\left\{1 - 2C_\lambda^{\,2}\cos(\phi)\right\} \quad (3)$$

which instantly reveals that the first order current amplitude variation term depends solely on the loop circumference in wavelengths. The loop current Eqn. (3) is valid for $C_\lambda < 0.3$, and is used to solve for the loop fields in classic fashion.

Figure 2 shows the loop current for the 2.85 m circumference loop at 7, 14, and 30 MHz, where C_λ is 0.067, 0.133, and 0.285 respectively. The variation increases with frequency.

1.3— General Form of the Loop Fields

With reference to the details in Note 5, the electric and magnetic fields are obtained from the vector **A** and scalar V potentials in classical fashion,

$$\mathbf{E} = -\nabla V - j\omega\mathbf{A} \quad (4)$$

$$\mathbf{H} = \frac{1}{\mu_0}\nabla\times\mathbf{A} \quad (5)$$

The boundary conditions require that tangential electric fields are zero on the loop surface everywhere except at the loop gap. The components of the vector potential in cylindrical coordinates are,

$$A_\phi = \frac{1}{4\pi}\iint_{S'} J_\phi\cos(\phi-\phi')GdS' \quad (6)$$

$$A_\rho = \frac{1}{4\pi}\iint_{S'} J_\phi\sin(\phi-\phi')GdS' \quad (7)$$

and the scalar potential is,

$$V = \frac{j\eta_0}{4\pi\varepsilon_0 k}\iint_{S'}\frac{1}{\rho'}\frac{\partial J_\phi}{\partial\phi'}GdS' \quad (8)$$

The integrals are over the surface S' of the loop wire. The intrinsic impedance of free space is η_0 Ω, and $k = 2\pi/\lambda$ m^{-1} is the wave number, and ε_0 F/m is the free space permittivity. The Green's function is,

$$G = \frac{e^{-jk|\mathbf{r}-\mathbf{r}'|}}{|\mathbf{r}-\mathbf{r}'|} \quad (9)$$

where $|\mathbf{r}-\mathbf{r}'|$ is the distance between the field point and the current density point on the wire. We solved these equations in a *Mathcad* spread sheet, and the details are available on the **www.arrl.org/qexfiles** web page. The results are valid from the surface of the loop conductor to everywhere in space. We also validated these analytical results with simulations using an NEC model rendered in 4*nec*2 software, see Table 1, also on the **/qexfiles** web page. The NEC model includes the primary loop, the secondary feeding loop, a length of wire representing the shield of the coax cable feed line, and a resonating capacitor.

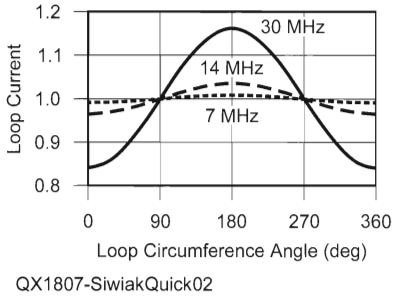

QX1807-SiwiakQuick02

Figure 2 — Loop currents at 7, 14, and 30 MHz along the loop circumference vary in amplitude due to the inclusion of a Fourier series expansion term.

Table 1.

Numerical Electromagnetic Code (4nec2) model includes the primary loop, a secondary feeding loop and segment of wire representing the shield of the coax cable feed line, and a resonating capacitor.

```
CM                                      Frequency - frq MHz
CM                                      Includes feed stub; (1+j0)V source
CM                                      RG-213/U primary loop, Rloss aluminum
CM                                      RG-58/U coupling loop
CM                                      No Ground
CE
SY frq=14.10                            'frequency MHz
SY b=0.45339                            'primary loop radius, m
SY a=0.004064                           'Primary loop wire radius, m
SY b2=0.077                             'Feed loop radius, m
SY a2=0.002                             'Feed loop wire radius, m
CM
SY C=43.40e-12                          'INPUT RESONATING CAPACITOR, Farad
CM
SY Qc=2400                              'Input resonating capacitor Q
SY Rp=Qc/(2*3.1415926535*frq*1e6*C)     'Parallel equivalent capacitor resistance
SY cond=34000000                        'aluminum, RC-213/U shield conductivity
SY n=64                                  'Input n-polygon primary loop
SY n2=16                                'Input n-polygon coupling loop
SY ang1b=-90-360/(2*n)                  'start of arc angle of primary loop
SY ang2b=ang1b+360                      'end of arc of primary loop
SY ang1b2=-90-360/(2*n2)                'start of arc angle of feed loop
SY ang2b2=ang1b2+360                    'end of arc angle of feed loop
SY zb=1.5                               'elevation in Z of center of loop
SY loopgap=4.5*(a+a2)                   'gap between primary and feed loop
SY zb2=zb+0.343038                      'elevation in Z of center of feed loop
CM
SY nstub=1                              'CHOOSE number of stub segments
CM                                      nstub=34 for 1.5 m cable; 74 for AlexLoop 129 inch coax length
SY stublength=0.0445*nstub              'compute stub 'SEGMENT LENGTH FIXED AT 0.0445 m
SY stubZ=1.7675                         'stub start coordinate
SY sEnd=stubZ-stublength                'stub end coordinate
CM                                      primary loop arc, GA, shifted in Z
GA   1  n      b                -0.0150219548  ang1b  ang2b  a
GM   0  0      0                0              0      0      0                0.03  zb     1
GA   2  n2     b2               -0.0150219548  ang1b2 ang2b2 a2
GM   0  0      0                0              0      0      0                0.03  zb2    2
CM
GW   3  1      -0.0150219548    0              stubZ  -0.0150219548  0.03  stubZ  a2
GW   4  nstub  -0.0150219548    0.03           stubZ  -0.0150219548  0.03  sEnd   a2
GE   0
LD   1  1      1                1              Rp     0              C
LD   5  0      0                0              cond
GN   -1
EK
EX   0  2      1                0              1.     0.0
FR   0  0      0                0              frq    0
EN
```

2 — Small Loop Impedance

The general form of the loop impedance with just radiation loss is,

$$Z_{loop} = \eta_0 \frac{\pi}{6}(kb)^4\left[1+8(kb)^2\right]\left[1-\frac{a^2}{b^2}\right]+\cdots$$
$$+j\omega\left[\mu_0 b\left[\ln\left(\frac{8b}{a}\right)-2+\frac{2}{3}(kb)^2\right]+M_{12}\right]\left[1+2(kb)^2\right] \quad (10)$$

including terms due to conductor thickness, and to the first-order current variation. The radian frequency is ω, and μ_0 is the free space permeability. M_{12} is the mutual coupling inductance between the primary and secondary loops obtained using the Neumann formula.

The *loaded* radiation Q of the antenna is,

$$Q_{rad} = \frac{1}{2}\frac{\mathrm{Im}\{Z_{loop}\}}{\mathrm{Re}\{Z_{loop}\}} \quad (11)$$

The primary loop loss resistance is,

$$R_{loss} = \frac{b}{a\delta\sigma} \quad (12)$$

where the σ is the loop conductivity in S/m, and the skin depth for good conductors is,

$$\delta = \sqrt{\frac{2}{\omega\mu_0\sigma}} \quad (13)$$

The Q_c of the resonating capacitor also contributes to losses in the form of parallel resistance across the capacitor, so that the net loaded Q_L of the antenna is,

$$Q_L = \frac{0.5}{\frac{1}{Q_C} + \frac{\mathrm{Re}\{Z_{loop}\} + R_{loss}}{\mathrm{Im}\{Z_{loop}\}}} \tag{14}$$

from which we can determine the loop current amplitude term I_0 for a given transmitter-supplied RF power P,

$$I_0 = \sqrt{\left(\frac{P}{R_{rad}}\right)\left(\frac{Q_L}{Q_{rad}}\right)} \tag{15}$$

The efficiency *eff* of the loop antenna follows as,

$$eff = \frac{I_0^{\,2} R_{rad}}{P} = \frac{Q_L}{Q_{rad}} \tag{16}$$

The value of Q_L can be obtained from Eqn. (14) or from direct measurements.

3 — The Secondary Feeding Loop

The secondary feeding loop has two main effects on the system. First, the total loop inductance increases by the mutual coupling inductance, M_{12}, between the primary loop and the secondary feeding loop. The result is that less capacitance is needed to resonate the antenna than if just the primary loop inductance were considered. Second, the relative diameters of the secondary feeding loop and the primary loop step up the primary loop resonant radiation plus loss resistance to the feed point value needed to match the feeding coax cable.

We used the Jordan and Balmain[10] high frequency extension to the Neumann formula, specialized to circular loops with constant current, to find the mutual coupling M_{12} between the primary loop and the secondary feeding loop.

$$M_{12} = \int_0^{2\pi}\int_0^{2\pi} \frac{b_2 b D_{12} \exp(-jkR_g)}{R_g} d\theta_1 d\theta_2 \tag{17}$$

and D_{12} and R_g are function of θ_1 and θ_2, the angles around the circumferences of the two loops,

$$D_{12} = \cos(\theta_1)\cos(\theta_2) + \sin(\theta_1)\sin(\theta_2) \tag{18}$$

and R_g further depends on the relative displacements of the two loops,

$$R_g = \sqrt{\left[b_2 \sin\theta_2 - b\sin\theta_1 + X\right]^2 + \cdots + \left[b_2 \cos\theta_2 - b\cos\theta_1 + Z\right]^2 + Y^2} \tag{19}$$

where X, Y, and Z are the center-to-center displacement distances of the two loops that are in the zx plane. We solved Eqn. (17) using direct numerical integration in *Mathcad* software and include that solution on the **/qex-files** web page. For our loop dimensions, $(L_{self}+M_{12})/L_{self}$ is 1.02. M_{11} is the self-inductance of the primary loop. M_{12} is 57.3 nH for our example, and the loop centers are displace in the loop plane by 0.343 m.

Eqn. (17) can also be used to compute the complex self inductance L_{self} of the primary loop. Then, $j\omega L_{self}$ provides another way to compute the primary loop radiation impedance and reactance for a constant loop current.

4 — Fields at the Loop Center and in the Far Field Null

The electric field perpendicular to the surface of the wire is proportional to the rate of change (differentiation) of the current in the circumferential ϕ direction around the loop. Since we've included a loop term that varies with $\cos(\phi)$, thus survives differentiation in ϕ, we can derive a expression for the electric field in the center of the loop plane. Likewise, we can analyze the far field of the loop in the far-field null direction. In both cases the solution originates with the $2(C_\lambda)^2\cos(\phi)$ term of the loop current.

4.1— Fields at the Loop Center

The electric field at the center of the loop in the zx plane is found from the derivative with respect to ϕ of the loop current. Stated at the loop center $(x, y, z) = (0, 0, 0)$,

$$E_\phi(0,0,0) = -j\frac{\eta_0 k I_0}{2} \tag{20}$$

and the magnetic field can be approximated from the single-turn solenoid equation,

$$H_z(0,0,0) = \frac{I_0}{2b}\ . \tag{21}$$

The electric field depends on wavelength (via k) but does not depend on any loop dimension. The magnetic field, however, depends on the loop radius b. The wave impedance Z_W at the loop center is a measure of how well the loop discriminates between the electric and magnetic fields. That wave impedance is,

$$Z_W = \frac{E_\phi}{H_z} = -j\eta_0 kb = -j\eta_0 C_\lambda \tag{22}$$

clearly revealing the dependence of Z_W on the loop circumference. Also, because the electric field at (0, 0, 0) depends on the *variation* in the loop current, we would not be able to formulate an expression for the wave impedance from just a constant current term.

4.2— The Far-field Null

We evaluated the fields very far from the antenna using the exact analytical expressions in *Mathcad* to determine the loop peak-to-null ratio, and validated the results by NEC simulations. The far-field peak-to-null ratio depends on the current variation term in a simple manner for $C_\lambda < 0.3$. Stated in decibels the peak-to-null ratio of the small loop is,

$$N_{dB} = -20\log(2C_\lambda) \tag{23}$$

Table 2 shows the null depth across the 7 to 30 MHz operating range of our example loop. We compared the null depth using the simple formula of Eqn. (23), a detailed loop near-field calculation in *Mathcad*, and the null calculated from the 4*nec*2 model. The null becomes monotonically and smoothly shallower as the frequency increases for a fixed-size loop. This is normal and expected; recall that at $C_\lambda = 1$ we have the popular full-wavelength loop that exhibits gain of about +4 dBi in the broadside direction. Omitting the current variation term results in an erroneous prediction of an infinitely deep null.

The formula and analysis rely on the first term of the current variation, while the NEC result calculates the exact loop current. The single additional Fourier term loop current approximation becomes less reliable as frequency increases, but is still viable up to 30 MHz. As a result, we estimate that our loop current including a single variation term is reasonably accurate up to at least $C_\lambda = 0.3$.

5 — Loop Coupling to the Coax Feed Line

The secondary loop is fed directly with unbalanced coaxial cable, so there is opportunity to generate common mode currents on the coax feed line. We modeled the primary loop, secondary loop and coax outer shield in 4*nec*2, as rendered in Figure 1. We then varied the length of the

Table 2.
The null depth becomes progressively shallower as the frequency increases.

f, MHz	Null [Eq. (23)], dB	Null [analysis], dB	Null [4nec2], dB
7	17.52	17.52	17.50
10	14.42	14.57	14.50
14	11.50	11.41	11.47
18	9.32	9.29	9.12
21	7.98	7.94	7.83
24	6.82	6.77	6.76
30	4.88	4.79	4.13

coax and searched for the maximum current on the coax cable shield, just like on a previous study involving common mode currents (CMC) on the feed line to a dipole[11] that lacked a current choke.

5.1 — Common Mode Currents on the Feed Line

In this loop antenna, the CMCs are generated at the connection of the coax feed directly to the secondary loop. The CMCs appear to end-feed the shield of the coax feed line. We would expect a maximum coupling to a half-wavelength long feed line. Indeed, Figure 3 shows that the maximum CMC occurs for a coaxial feed line length of 0.45 λ.

We considered a loop that had a fixed coaxial cable length of about 3.3 m — or 0.08 λ at 7 MHz and 0.33 λ at 30 MHz — so if a common mode choke were to be used, it should be located on the coax cable at least a loop diameter away from the loop antenna, perhaps somewhere between 0 and 1.5 m from the transmitter end of the 3.3 m long coax cable.

5.2 — Measuring Loop Currents

We attempted to measure the loop currents and the feed line CMC at 14 and 28 MHz for the loop with its 3.28 m coaxial feed cable, and for an extended cable 9.61 m in length, as close as we could get to 0.452 wavelengths at 14 MHz, the length corresponding to a peak current in Figure 3. One of us, (W4RQ) constructed a 2.5 cm diameter current probe for the task.

We were able to measure in the 20 m band that the primary loop current was stronger than the feed loop current, and that the primary loop current varies along the circumference with the upper half of the loop (near the secondary feeding loop, 180° in Figure 2) having a slightly greater value than the lower half.

Due to the relative insensitivity of our homebrew *H*-field probe, we found no discernible CMCs on the feed-line, either for a long (9.61 m) or short (3.28 m) coaxial cable. With the long (nearly λ/2) feed line length, the loop tuning was exceptionally "touchy" and unstable.

6 — Vertical Loop Coupling to the Ground

We used the Neumann formula, Eqn. (17) with b_2 set to b, and a displacement between the loops to resemble a loop center-to-center distance to its image in the ground. We estimated the loop coupling to the ground by calculating the mutual inductance between the primary loop and its image in the ground, normalized to the loop self inductance and expressed in percent. That coupling affects the impedance of the loop antenna system. There is also a ground reflection, quite apart from the mutual coupling to ground, that affects the radiation pattern in the elevation plane. Here we are concerned only with the mutual coupling term that affects impedance.

Placing the loop above a perfect electric conducting (PEC) ground results in the strongest coupling. We also estimated the coupling for the "average" ground (σ = 0.005 S/m, ε_r = 13), and to a "poor" ground (σ = 0.001 S/m, ε_r = 5), by reducing the PEC coupling by the magnitude of the refection coefficient for normal incidence on the ground. The reflection coefficient magnitude is 1.0 for the PEC ground, 0.593 for the "average" ground and 0.393 for "poor" ground dielectric parameters at 14.1 MHz. Figure 4 shows the ratio of the mutual coupling to the self inductance in percent, a measure of ground coupling analogous to the ratio of mutual impedance to self impedance for a vertical dipole above ground.

Even for a PEC ground the coupling is less than 0.5% for a loop with its center more than one loop diameter above ground — where the bottom of the loop is a loop radius above ground. Using parameters for "real" ground further reduces that apparent mutual coupling. A loop with its center more than one loop diameter above ground is essentially independent of ground coupling as far as the effect on impedance and loop tuning is concerned. Note that ground reflections, quite apart from ground coupling, do have a significant effect on the loop antenna patterns.

7 — Efficiency of the Small Loop

We compared three methods to estimate the radiation efficiency of the small loop. In one *calculated* method we analytically determined the total loaded Q_L using Eqn. (14) and compared that to the loaded Q_{rad} of Eqn. (11), and then applied Eqn. (16) for the efficiency.

In a second method we measure *loaded* Q_L using a matched transmitter, and the classic bandwidth formula,

$$Q_L = \frac{\sqrt{F_H F_L}}{F_H - F_L} = \frac{\text{Frequency}}{\text{Bandwidth}} \tag{24}$$

where, given the antenna impedance, $Z = R + jX$ then F_H is the

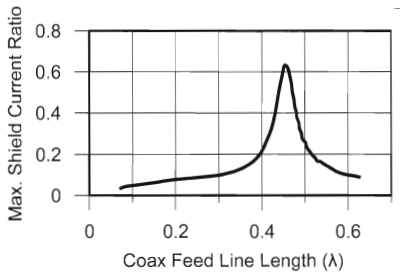

Figure 3 — Simulations using an NEC model of the loop antenna system of Figure 1 show that the maximum common mode current on the feeding cable has a strong but narrow peak for cable lengths that are near the half-wave resonant length.

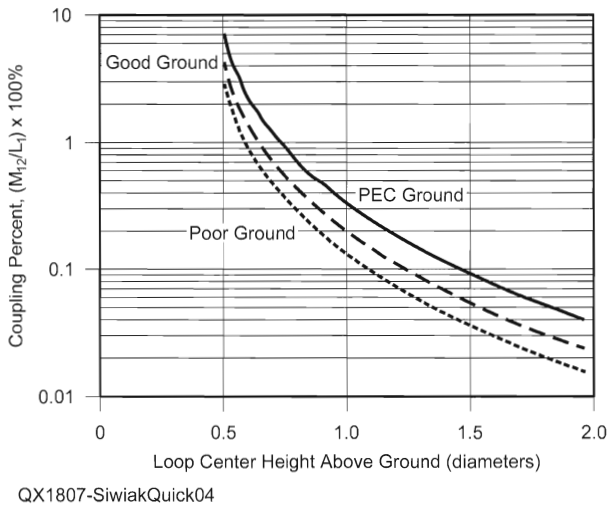

Figure 4 — The percent coupling to ground for this small HF loop is insignificant when the loop center is at least one loop diameter above the ground. Coupling is strongest for a PEC ground, and decreases significantly for realistic ground parameters.

frequency where $R = X$, and F_L is where $R = -X$, so that $F_H - F_L$ is the 3 dB bandwidth. F_H and F_L correspond to the 2.236:1 VSWR and the 7 dB return loss points. When the reactance does not cross zero, we can apply the incremental impedance formula,

$$Q = \frac{f}{2}\frac{|\Delta Z/\Delta f|}{R} \tag{25}$$

where for a small antenna, $|\Delta Z/\Delta f|$ is the magnitude of the incremental change in impedance Z divided by the incremental change in frequency f; and R is the resistance, or $\mathrm{Re}\{Z\}$ at frequency f. We then applied Eqn. (16) for the efficiency. These two approaches are the Q-method[12] for measuring efficiency.

Finally, we used the NEC model to simulate the efficiency. Figure 5 shows that all three methods of determining efficiency are within 0.5 dB of each other across 7 to 29 MHz, inspiring confidence in the analysis and in the NEC model.

The loop loss and radiation resistances increase with frequency. When resonated by the tuning capacitor, and transformed by mutual coupling to the feeding loop, the result is nearly constant input impedance across the operating frequencies. This is one of the key characteristics taught by Dunlavy in his 1971 patent. The secondary loop diameter and location bear an optimum relationship to the diameter of the primary loop so that variation in feed impedance is minimized over the band of operation.

8 — Conclusions

We introduced new improved formulas for the small HF loop current, and for the loop impedance by including one additional term of the Fourier series expansion for the loop current. That term is needed to adequately describe the current for loops up to 0.3 wavelengths in circumference. Including the additional Fourier term results in simple and accurate expressions for (1) the ratio of the electric-to-magnetic fields (field impedance Z_W) at the exact center of the loop, and (2) the far-field null depth.

CMCs on the feed line are small (negligible) as long as the feeding coax cable is not longer than the 3.3 m (less than 0.33 λ at the upper frequency extreme) length supplied with our example loop. CMC chokes, if used, could be attached between the transmitter end of the coax and up to 1.5 m from the transmitter end of the 3.3 m long cable.

Coupling of the vertical loop to a PEC ground is small, and decreases for realistic ground parameters, especially if the loop center is at least a loop diameter above ground. The loop coupling to ground, distinct from ground reflections that affect the elevation patterns, affects only the impedance match, which then requires a very small retuning of the loop.

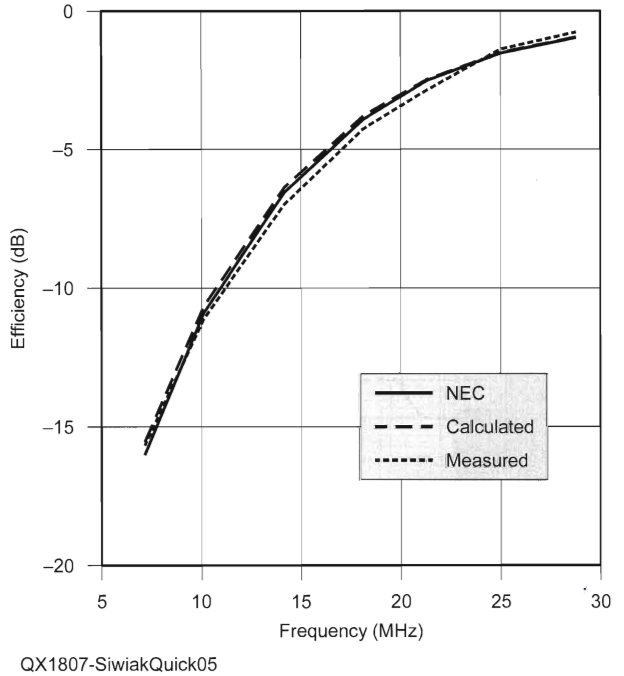

Figure 5 — Small loop efficiency simulated in NEC (solid), calculated from loop equations (long dashes), and measured using the Q method (short dashes). The close agreement among three methods validates the analysis, the Q measurements, and the completely independent NEC model.

Kazimierz (Kai) Siwiak, KE4PT, earned his PhD from Florida Atlantic University, Boca Raton, FL, specializing in antennas and propagation. He is a registered Professional Engineer and Life Senior Member of IEEE. Dr. Siwiak holds 41 US patents, has authored many peer-reviewed papers, several textbooks, and has contributed chapters to other books. Kai holds an Amateur Extra class license, is a life member of AMSAT, and member of ARRL where he serves on the RF Safety Committee and as Technical Advisor. He is a QST Contributing Editor, and Editor of QEX. Kai is a dedicated DXer and enjoys portable operating. His interests include flying (instrument and multiengine commercial pilot), hiking, and camping.

Richard Quick, W4RQ, is a retired Electronics and Metrology Engineering Technician. He was first licensed in 1977, and now holds the Amateur Extra class license. Richard is a member of the ARRL. He has built and tested several small loop transmitting antennas, studying the effects of using various materials and components, and has modeled them using Numerical Electromagnetic Code. Richard has co-authored the articles, "Does Your Antenna Need a Choke or Balun?" (QST, March 2017) and "Live Trees Affect Antenna Performance" (QST, February 2018). Richard enjoys operating at low power levels and from portable locations. He is an avid CW operator.

Notes

[1]John H. Dunlavy, Jr., "Wide Range Tunable Transmitting Loop Antenna", *US Patent 3,388,905*, issued June 28, 1971.
[2]H. C. Pocklington, "Electrical oscillations in wires," *Proc. Cambridge Phil. Soc.*, vol. 9, pp. 324-333, 1897.
[3]E. Hallén, "Theoretical investigation into transmitting and receiving qualities of antennae," *Nova Acta Regiae Soc. Ser. Upps.*, vol. II, pp. 1-4 , Nov. 4, 1938.
[4]J. E. Storer, "Impedance of thin-wire loop antennas," *Trans. AIEE*, vol. 75, pp. 606-619, Nov. 1956.
[5]Q. Balzano and K. Siwiak, "The Near Field of Annular Antennas," *IEEE Trans. Veh. Tech.*, Vol. VT-36, Nov. 1987, pp. 173-184.
[6]K. Siwiak, "Loop Antennas," in John G. Proakis (Ed.), **Wiley Encyclopedia of Telecommunications**, New York, NY: John Wiley & Sons, 2002, pp. 1290-1299.
[7]F. E. Neumann, "Allgemeine Gesetze der inducirten elektrischen Ströme [General laws of electrically induced currents]", *Treatises of the Royal Academy of Sciences in Berlin, Annalen der Physik*, 1846, vol. 143, issue 1, pp. 31-44.
[8]The *4nec2* NEC based antenna modeler and optimizer, by Arie Voors, **www.qsl.net/4nec2**.
[9] P. Salas, AD5X, Short Takes: The AlexLoop Walkham Portable Antenna, *QST*, Nov., 2013, p. 67.
[10]E.C. Jordan and K. G. Balmain, Section 14.16, p. 598, **Electromagnetic Waves and Radiating Systems, Second Edition**, Prentice–Hall, Inc., Englewood Cliffs, NJ.
[11]R. Quick, W4RQ, and K. Siwiak, KE4PT, "Does Your Antenna Need a Choke or a Balun?", *QST*, Mar, 2017, pp. 30-33.
[12]A. Findling, K9CHP and K. Siwiak, KE4PT, "How Efficient is Your QRP Small Loop Antenna?", *QRP Quarterly*, Summer 2012.
[13]K. Siwiak, KE4PT, "Q and the Energy Stored Around Antennas", *QST*, Feb., 2013, pp 37-38.